EPJ manuscript No.
(will be inserted by the editor)

Shell-structure fingerprints of tensor interaction

M. Zalewski[1], W. Satuła[12], J. Dobaczewski[13], P. Olbratowski[1], M. Rafalski[1], T. R. Werner[1], and R. A. Wyss[2]

[1] Institute of Theoretical Physics, University of Warsaw, ul. Hoża 69, 00-681 Warsaw, Poland
[2] KTH (Royal Institute of Technology), AlbaNova University Center, 106 91 Stockholm, Sweden
[3] Department of Physics, P.O. Box 35 (YFL), FI-40014 University of Jyväskylä, Finland

Received: November 25, 2008/ Revised version: November 25, 2008

Abstract. We address consequences of strong tensor and weak spin-orbit terms in the local energy density functional, resulting from fits to the $f_{5/2} - f_{7/2}$ splittings in ^{40}Ca, ^{48}Ca, and ^{56}Ni. In this study, we focus on nuclear binding energies. In particular, we show that the tensor contribution to the binding energies exhibits interesting topological features closely resembling that of the shell-correction. We demonstrate that in the extreme single-particle scenario at spherical shape, the tensor contribution shows tensorial magic numbers equal to $N(Z)$=14, 32, 56, and 90, and that this structure is smeared out due to configuration mixing caused by pairing correlations and migration of proton/neutron sub-shells with neutron/proton shell filling. Based on a specific Skyrme-type functional SLy4$_T$, we show that the proton tensorial magic numbers shift with increasing neutron excess to Z=14, 28, and 50.

PACS. 21.60.Jz Nuclear Density Functional Theory and extensions (includes Hartree-Fock and random-phase approximations) 21.60.-n Nuclear structure models and methods

1 Introduction

Density functional theory (DFT) is a universal *ab initio* approach designed and used to calculate properties of electronic systems entrapped in the external Coulomb field of nuclei. It has been successfully applied to atoms, molecules, or condensed media. Universality of the DFT means independence of a functional form of the shape of external one-body potential holding the electronic system together. The existence of such a universal and, in principle, exact density functional describing ground-states of externally bound fermionic systems is guaranteed by the Hohenberg-Kohn [1] and Kohn-Sham [2] (HKS) theorems.

Generalization of the DFT theory to self-bound systems like atomic nuclei encounters problems associated with intrinsic rather than laboratory density which characterizes the atomic nuclei, see Ref. [3,4,5]. In spite of that, the HKS theorem have strongly influenced the way of thinking in the field of nuclear structure. Nowadays, the nuclear structure theorists employ the functionals that are treated as separate entities, independently, to a large extent, of the underlying effective nucleon-nucleon (NN) interactions like, for example, the local Skyrme interaction [6]. Free parameters of these functionals are directly adjusted to fit empirical data. There are also attempts to enrich their functional form as compared to the form resulting from the mean-field (MF) averaging of the effective Skyrme interaction [7], which are motivated by a rather mediocre performance of the conventional Skyrme-type functionals, see for example Refs. [8,9].

Adequateness of the fitting strategy – that is, the choice of the data set – is a key factor determining performance of the nuclear energy density functional (EDF) method. In this work we explore the Skyrme-type local EDF approach to nuclear structure and focus on the spin-orbit (SO) and tensor parts of the functional. Throughout the years, not much attention was paid to, in particular, the tensor part, mainly due to the lack of clear experimental data constraining the strength of this part of the EDF. Hence, the tensor term in the existing Skyrme functionals is either trivially set to zero by hand, see the review in Ref. [10], or is a result of a global fit to bulk nuclear properties [11].

Recent revival of interest in the tensor term was triggered by systematic observation of non-conventional shell evolution in isotopic chains of light nuclei far from stability, including new magic shell-gap opening at N=32, see for example Refs. [12,13]. Otsuka and collaborators associated these effects with the two-body tensor interaction [14, 15]. This interpretation was soon confirmed within the local Skyrme-type EDF models [16,17,18,19,20,21]. Inclusion of single-particle (s.p.) energies in the fitting data sets appears to lead to the tensor coupling constants [17,20,21, 22,23,24] which are at variance with bulk fits, see Fig. 1 and extensive discussion in Ref. [11].

The aim of this work is to look into consequences of strong attractive isoscalar and isovector tensor fields and weak SO fields resulting from the fitting method proposed by our group [22]. In particular, we study such consequences for the nuclear binding energies. The paper is

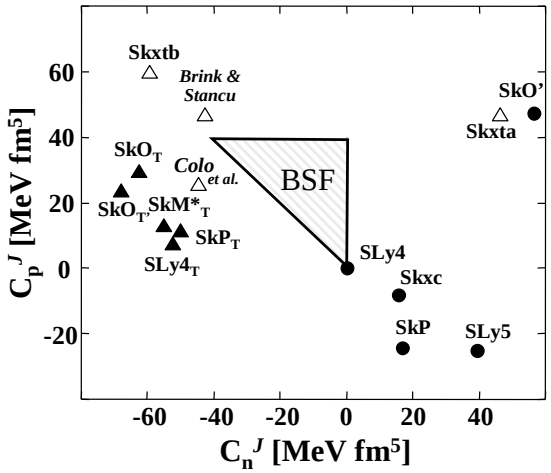

Fig. 1. Proton $C_p^J = (C_0^J - C_1^J)/2$ versus neutron $C_n^J = (C_0^J + C_1^J)/2$ tensor coupling constants resulting form fits to: bulk nuclear properties (black dots) and the s.p. levels and the SO splittings (triangles). Open triangles represent fits of Ref. [17, 20,21]. Black triangles mark our results [22,23,24] from the fit to the $f_{7/2} - f_{5/2}$ SO splittings. Shaded area represents the parameters established by Brink, Stancu and Flocard (BSF) in their seminal paper [25]
.

organized as follows. In Sec. 2, theoretical framework is briefly outlined. In Sec. 3, the procedure used to fit the tensor and SO coupling constants is discussed. In Sec. 4, numerical results showing tensor energy contribution to the total binding energy, followed by a discussion of *tensorial magic structure*, is presented. The paper is summarized in Sec. 5.

2 Tensor and spin-orbit parts of the local nuclear energy density functional

In this work we consider the local EDF $\mathcal{H}(\mathbf{r})$ of the Skyrme-type. It consists of a kinetic energy and a sum of isoscalar (t=0) and isovector (t=1) potential energy terms:

$$\mathcal{H}(\mathbf{r}) = \frac{\hbar^2}{2m}\tau_0 + \sum_{t=0,1}\Big\{\mathcal{H}_t(\mathbf{r})^{\rm even} + \mathcal{H}_t(\mathbf{r})^{\rm odd}\Big\}, \qquad (1)$$

where

$$\mathcal{H}_t^{\rm even} = C_t^{\rho}[\rho_0]\rho_t^2 + C_t^{\Delta\rho}\rho_t\Delta\rho_t + C_t^{\tau}\rho_t\tau_t + C_t^J\mathbb{J}_t^2 + C_t^{\nabla J}\rho_t\nabla\cdot\mathbf{J}_t, \qquad (2)$$

$$\mathcal{H}_t^{\rm odd} = C_t^{s}[\rho_0]\mathbf{s}_t^2 + C_t^{\Delta s}\mathbf{s}_t\cdot\Delta\mathbf{s}_t + C_t^{T}\mathbf{s}_t\cdot\mathbf{T}_t + C_t^{j}\mathbf{j}_t^2 + C_t^{\nabla j}\mathbf{s}_t\cdot(\nabla\times\mathbf{j}_t), \qquad (3)$$

with the density-dependent primary coupling constants $C_t^{\rho}[\rho_0]$ and $C_t^{s}[\rho_0]$. The potential energy terms are bilinear forms of either time-even (ρ, τ, $\mathbb{J}$) or time-odd ($\mathbf{s}$, $\mathbf{j}$, $\mathbf{T}$) densities and their derivatives, see, e.g.. Ref. [10] for details. The $\mathbf{J}_t$ density denotes the vector part of the spin-current tensor, $\mathbf{J}_{t,\lambda} = \sum_{\mu\nu}\epsilon_{\lambda\mu\nu}\mathbb{J}_{t,\mu\nu}$.

In this work we focus on the tensor,

$$\mathcal{H}^T = C_0^J\mathbb{J}_0^2 + C_1^J\mathbb{J}_1^2, \qquad (4)$$

and the SO terms,

$$\mathcal{H}^{SO} = C_0^{\nabla J}\rho_0\nabla\cdot\mathbf{J}_0 + C_1^{\nabla J}\rho_1\nabla\cdot\mathbf{J}_1. \qquad (5)$$

In the limit of spherical symmetry, the vector part $\mathbf{J}_t \equiv J_t(r)\mathbf{e}_r$ is the only non-vanishing part of the tensor density $\mathbb{J}_{\mu\nu}$. Hence, in this limit, the tensor part of the functional (4) reduces to:

$$\mathcal{H}^T = \frac{1}{2}C_0^J\mathbf{J}_0^2 + \frac{1}{2}C_1^J\mathbf{J}_1^2. \qquad (6)$$

By performing variation of the functional with respect to $J_t(r)$ one obtains the one-body SO potential:

$$W_t^{SO} = -\frac{1}{2r}\left(C_t^{\nabla J}\frac{d\rho_t}{dr} - C_t^J J_t(r)\right)\mathbf{L}\cdot\mathbf{S}, \qquad (7)$$

which is composed of two terms. The first term is coming form the SO term in the functional, Eq. (5). It is proportional to the radial derivative of the particle density and is relatively slowly varying with N and Z. The second component is due to the tensor term (4). It is proportional to the SO density $J_t(r)$ which is strongly shell-filling dependent. Indeed, in the spherical symmetry limit, the SO vector density can be written as [26]:

$$J(r) = \frac{1}{4\pi r^3}\sum_{n,j,l}(2j+1)v_{njl}^2 \times\left[j(j+1) - l(l+1) - \frac{3}{4}\right]\psi_{njl}^2(r), \qquad (8)$$

where v_{njl}^2 and $\psi_{njl}^2(r)$ are occupation probabilities and radial wave functions, respectively, of states with given quantum numbers. If both SO partners $j_{\gtrless} = l \pm 1/2$ are fully occupied, i.e., when the system is spin-saturated (SS) the $J(r)$ density vanishes. Examples of the SS systems include ^{16}O, ^{40}Ca, or ^{80}Zr at spherical shape. Most of the nuclei are spin-unsaturated (SUS). The SO vector density reaches its maximum when one (or more) of the SO partners is fully occupied while the other one is completely empty.

3 Fitting procedure

Fitting procedure used to constrain the coupling constants C_t^J and $C_t^{\nabla J}$ was described in detail in Ref. [22] and we only recall it here very briefly. The idea is to reproduce experimental $f_{7/2} - f_{5/2}$ SO splittings in three key nuclei: ^{40}Ca, ^{48}Ca, and ^{56}Ni. Since ^{40}Ca is, as discussed above, a SS system, the conventional SO term of Eq. (5) is the

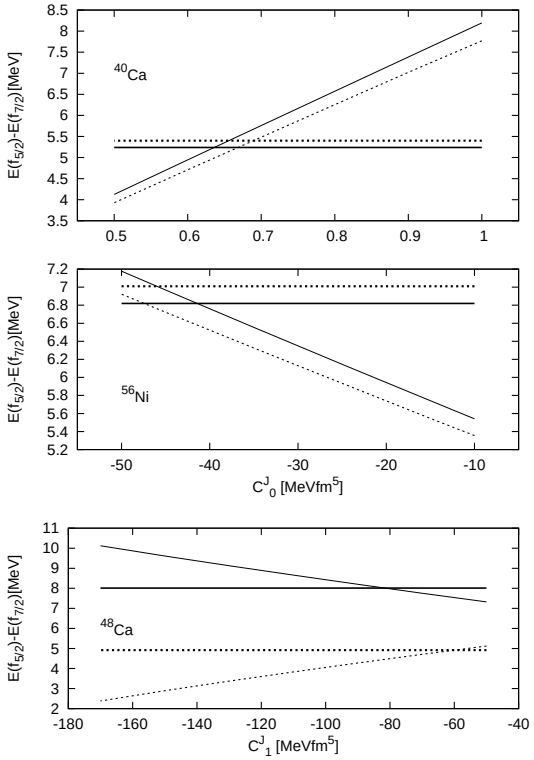

Fig. 2. Empirical (horizontal lines) and theoretical (inclined lines) $f_{7/2}-f_{5/2}$ splittings in ^{40}Ca, ^{48}Ca, and ^{56}Ni as a function of $C_0^{\nabla J}/C_0^{\nabla J}$(SLy4) (upper panel), C_0^J (middle panel), and C_1^J (lower panel). Solid an dashed lines represent neutron an proton splittings, respectively. The theoretical results are obtained by modifying the SO and tensor strengths in the SLy4 functional. Empirical data are taken from [27]. See text for further details.

only source of the SO splitting. Hence, this nucleus is used to set the isoscalar strength of the SO term $C_0^{\nabla J}$. Having set $C_0^{\nabla J}$, we next constrain the C_0^J strength by using the $f_{7/2} - f_{5/2}$ SO splitting in the isoscalar ($N = Z$) SUS nucleus ^{56}Ni. Finally, we move to ^{48}Ca, where protons and neutrons constitute a SS and SUS system, respectively. This nucleus is used to fit the isovector coupling constants or, more precisely, to fit $C_1^{\nabla J}$, because the ratio $C_0^{\nabla J}/C_1^{\nabla J}$ is kept equal to the value characteristic for the given Skyrme parametrization. There is one piece of data on the $f_{7/2} - f_{5/2}$ SO splittings, preferably in ^{48}Ni or ^{78}Ni, which is badly needed to fit the tensor and SO terms uniquely.

The procedure outlined above is illustrated in Fig. 2 for the case of the SLy4 functional [28] but it is qualitatively independent of the initial parameterization. As shown in the figure, a good agreement with empirical data requires, for this low-effective-mass force, circa 35% reduction of $C_0^{\nabla J}$ as compared to the original value, a large attractive isoscalar tensor coupling constant $C_0^{\nabla J}$ of about $-45\,\mathrm{MeV\,fm^5}$, and $C_1^{\nabla J}$ of about $-70\,\mathrm{MeV\,fm^5}$. It appears that the resulting tensor coupling constants $C_t^{\nabla J}$ (as well as the SO strengths C_0^J) are, to large extent, independent on the initial parameterization. This is illustrated in Fig. 1 where different functionals modified according to our prescription, see Refs. [22,23,24], are collected. They are labeled by a subscript T following the force acronym and marked by black triangles.

4 Contribution from the tensor terms to the binding energy

Fig. 3 shows the contribution to the total nuclear binding energy due to the tensor term, calculated by using the spherical Hatree-Fock-Bogolubov (HFB) code HFBRAD [29] with the SLy4$_T$ functional. Contributions due to the isovector and isoscalar parts are depicted separately in the upper and middle panels, respectively. The total contribution, $B_T(N,Z)$, is shown in the lowest panel of the figure.

From these results one can see that the isovector component is rather weak. Hence, the topology of the total contribution to the energy is mostly determined by the isoscalar term that shows a strong shell dependence. Following the argumentation presented in Sec. 2, the strongest tensor effects are expected to appear for $N(Z)$=14, 32, 56, and 90. They correspond to nucleons filling the $1d_{5/2}$, $1f_{7/2} \oplus 2p_{3/2}$, $1g_{9/2} \oplus 2d_{5/2}$ and $1h_{11/2} \oplus 2f_{7/2}$ shells, respectively, which creates a maximum SUS filling. Hence, these numbers can be regarded as *tensorial magic numbers*.

However, as it is seen from Fig.(3), the $B_T(N,Z)$ does not follow the expected pattern exactly. This is due to (*i*) pairing-induced configuration mixing and (*ii*) changes in the s.p. ordering of levels caused by the combination of strong attractive tensor fields and strongly reduced SO field. Two such situations are visible in Fig. 3. For $N < 30$ the tensor contribution is, as expected, largest for $_{32}$Ge. For $40 < N < 50$, however, the minimum on the plot is shifted toward the $_{28}$Ni isotopes, which suggests a change in the order of the $1p_{3/2}$ and $1f_{5/2}$ proton sub-shells with increasing neutron excess. The figure also indicates that on the proton side, $Z = 50$ rather than $Z = 56$ is the tensorial magic number. Again, this suggests that the $1g_{7/2}$ proton sub-shell is filled before $1d_{5/2}$. Consequently, the tensorial magic numbers may slightly differ for neutrons ($N = 14$, 32, and 56) and for protons ($Z = 14$, 28, and 50). This effect, however, may strongly depend upon a rather delicate balance between the tensor and SO strengths and needs to be studied in detail.

5 Summary

A new strategy of fitting the coupling constants of the nuclear energy density functional was recently proposed by our group [22]. It is based on a fit of the isoscalar spin-orbit and both isoscalar and isovector tensor coupling constants directly to the the $f_{5/2} - f_{7/2}$ SO splittings in ^{40}Ca, ^{56}Ni, and ^{48}Ca. Our results show that drastic changes in the isoscalar SO strength and the tensor coupling constants

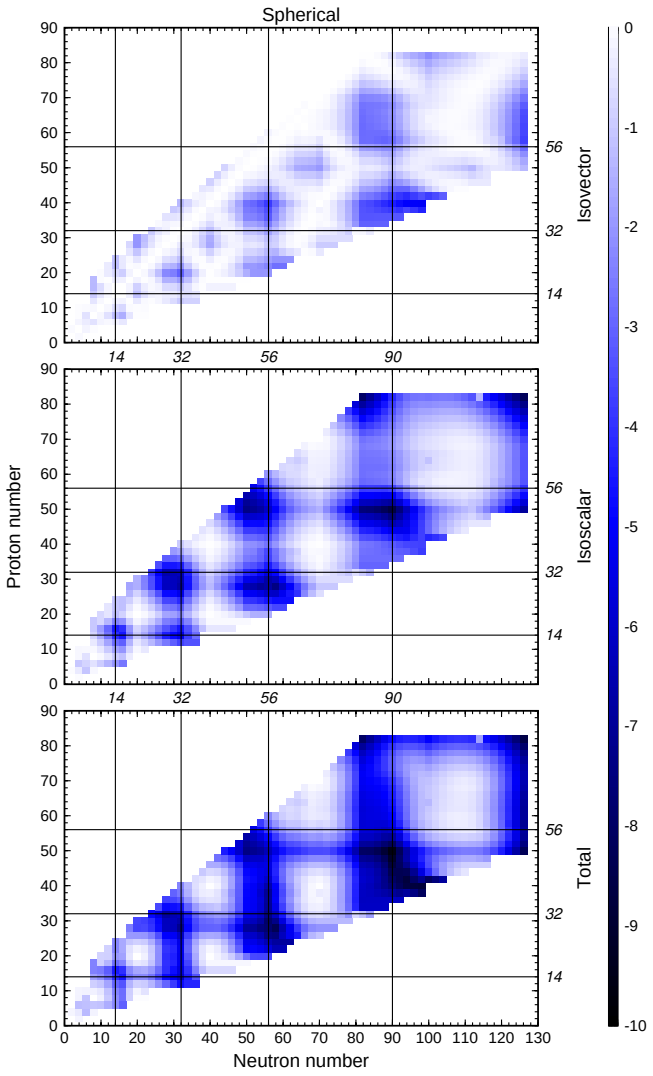

Fig. 3. The isovector (upper), the isoscalar (middle) and the total (lower) tensor contribution to the nuclear binding energy. The calculations were done using the SLy4$_T$ interaction in the particle-hole channel and the volume-δ interaction in the particle-particle channel with spherical symmetry assumed. Vertical and horizontal lines indicate the single-particle tensorial magic numbers at spherical shape. See text for further details.

are required as compared to the commonly accepted values

This work briefly addresses the consequences of strong attractive tensor and weak SO fields on binding energies. In particular, a contribution to the binding energy due to the tensor interaction is calculated. It shows a generic pattern closely resembling that of the shell-correction. The *tensorial magic numbers* are shifted up relatively to the standard magic numbers, towards $N(Z)$=14, 32, 56, or 90, which, in the extreme s.p. scenario at the spherical shape, correspond to the maximum spin-orbit asymmetry in the $1d_{5/2}$, $1f_{7/2} \oplus 2p_{3/2}$, $1g_{9/2} \oplus 2d_{5/2}$, and $1h_{11/2} \oplus 2f_{7/2}$ configurations, respectively. It is shown that these numbers are smeared out by the pairing effects and shifted in the case of protonic tensorial magic numbers by changes in the sub-shell ordering. It is also shown that strong attractive tensor interaction may give rise to an increased stability of nuclear binding at the drip lines, in particular around $Z \approx 14, N \approx 32$, $Z \approx 28, N \approx 56$, and $Z \approx 50, N \approx 90$.

This work was supported in part by the Polish Ministry of Science under Contract No. N N202 328234, by the Academy of Finland and University of Jyväskylä within the FIDIPRO programme, and by the Swedish Research Council.

References

1. P. Hohenberg and W. Kohn, Phys. Rev. **136**, B864 (1964); M. Levy, Proc. Nat. Acad. Sci. **76**, 6062 (1979).
2. W. Kohn and L.J. Sham, Phys. Rev. **140**, A1133 (1965).
3. J. Engel, Phys. Rev. C **75**, 014306 (2007).
4. B.G. Giraud, Phys. Rev. **C77**, 014311 (2008).
5. B.G. Giraud, B.K. Jennings, and B.R. Barrett, Phys. Rev. **A78**, 032507 (2008).
6. T.H.R. Skyrme, Phil. Mag. **1** (1956) 1043; Nucl. Phys. **9** (1959) 615.
7. B.G. Carlsson, J. Dobaczewski, and M. Kortelainen, LANL e-print arXiv:0807.4925.
8. M. Kortelainen, J. Dobaczewski, K. Mizuyama, and J. Toivanen, Phys. Rev. C **77**, 064307 (2008).
9. P. Klüpfel, P.-G. Reinhard, J. A. Maruhn, arXiv:0804.3402.
10. M. Bender, P.-H. Heenen, and P.-G. Reinhard, Rev. Mod. Phys. **75**, 121 (2003).
11. T. Lesinski, M. Bender, K. Bennaceur, T. Duguet, and J. Meyer, Phys. Rev. **C76**, 014312 (2007).
12. B. Fornal, S. Zhu, R.V.F. Janssens, M. Honma, R. Broda, P.F. Mantica, B.A. Brown, M.P. Carpenter, P.J. Daly, S.J. Freeman, Z.W. Grabowski, N.J. Hammond, F.G. Kondev, W. Krolas, T. Lauritsen, S.N. Liddick, C.J. Lister, E.F. Moore, T. Otsuka, T. Pawlat, D. Seweryniak, B.E. Tomlin, and J. Wrzesinski, Phys. Rev. C **70**, 064304 (2004).
13. D.-C. Dinca, R.V.F. Janssens, A. Gade, D. Bazin, R. Broda, B.A. Brown, C.M. Campbell, M.P. Carpenter, P. Chowdhury, J.M. Cook, A.N. Deacon, B. Fornal, S.J. Freeman, T. Glasmacher, M. Honma, F.G. Kondev, J.-L. Lecouey, S.N. Liddick, P.F. Mantica, W.F. Mueller, H. Olliver, T. Otsuka, J.R. Terry, B.A. Tomlin, and K. Yoneda, Phys. Rev. C **71**, 041302 (2005).
14. T. Otsuka, T. Suzuki, R. Fujimoto, H. Grawe, and Y. Akaish, Phys. Rev. Lett. **95**, 232502 (2005).
15. T. Otsuka, T. Matsuo, and D. Abe, Phys. Rev. Lett. **97**, 162501 (2006).
16. J. Dobaczewski, in Proceedings of the *Third ANL/MSU/INT/JINA RIA Theory Workshop: Opportunities with Exotic Beams*, Argonne, USA, April 4-7, 2006, eds. T. Duguet, H. Esbensen, K.M. Nollet, and C.D. Roberts (World Scientific, Singapore, 2007), p. 152, nucl-th/0604043.
17. B.A. Brown, T. Duguet, T. Otsuka, D. Abe, and T. Suzuki, Phys. Rev. C **74**, 061303(R) (2006).
18. J. Dobaczewski, N. Michel, W. Nazarewicz, M. Płoszajczak, and J. Rotureau, Prog. Part. Nucl. Phys. **59**, 432 (2007).

19. S. Sugimoto, K. Ikeda, and H. Toki, Phys. Rev. C **75**, 014317 (2007).
20. G. Colo, H. Sagawa, S. Fracasso, and P.F. Bortignon, Phys. Lett. **B646**, 227 (2007).
21. D.M. Brink and Fl. Stancu, Phys. Rev. **C75**, 064311 (2007).
22. M. Zalewski, J. Dobaczewski, W. Satuła, and T.R. Werner, Phys. Rev. **C77**, 024316 (2008).
23. W. Satuła, R.A. Wyss and M. Zalewski, Phys. Rev. **78**, 011302(R) (2008).
24. M. Zalewski *et al.*, in preparation.
25. D. Brink, Fl. Stancu, and H. Flocard, Phys. Lett. **B68**, 108 (1977).
26. D. Vautherin and D.M. Brink, Phys. Rev. C **5**, 626 (1972).
27. A. Oros, Ph.D. thesis, University of Köln, 1996.
28. E. Chabanat, P. Bonche, P. Haensel, J. Meyer, and R. Schaeffer, Nucl. Phys. **A627** (1997) 710; **A635** (1998) 231.
29. K. Bennaceur and J. Dobaczewski, Comput. Phys. Commun. **168**, 96 (2005).